Astrocytic regulation of cortical UP states

Kira E. Poskanzer[1] and Rafael Yuste

Howard Hughes Medical Institute and Department of Biological Sciences, Columbia University, New York, NY 10027

Edited* by Marcus E. Raichle, Washington University, St. Louis, MO, and approved September 27, 2011 (received for review July 29, 2011)

The synchronization of neuronal assemblies during cortical UP states has been implicated in computational and homeostatic processes, but the mechanisms by which this occurs remain unknown. To investigate potential roles of astrocytes in synchronizing cortical circuits, we electrically activated astrocytes while monitoring the activity of the surrounding network with electrophysiological recordings and calcium imaging. Stimulating a single astrocyte activates other astrocytes in the local circuit and can trigger UP state synchronizations of neighboring neurons. Moreover, interfering with astrocytic activity with intracellular injections of a calcium chelator into individual astrocytes inhibits spontaneous and stimulated UP states. Finally, both astrocytic activity and neuronal UP states are regulated by purinergic signaling in the circuit. These results demonstrate that astroglia can play a causal role in regulating the synchronized activation of neuronal ensembles.

cortex | electrophysiology | glia | sleep | two-photon

The transient synchrony of distributed groups of neurons is an important operational characteristic of the cerebral cortex for sensory processing and internal computational functions (1–4). One important type of synchrony—the multineuronal, network-driven fluctuations in membrane potential known as UP and DOWN states—occurs in neocortex both in vitro and in vivo (5–11). During UP states, neurons are depolarized for up to hundreds of milliseconds, sometimes firing barrages of action potentials (12). The function of these UP states is unknown, although they underlie synchronization among distant cortical territories (13). UP states in vivo are observed at similar frequencies as the "resting" spontaneous activity that is evident in functional MRI and EEG recordings from human subjects when not involved in sensory motor tasks (14–16), so they may be a cellular basis of this activity.

The mechanisms by which UP states occur remain unclear, although recurrent excitatory activity is important (6, 9). Because astrocytes regulate extracellular glutamate (17), we explored their effects on cortical UP states using electrophysiology and population calcium imaging. The effects of astroglia on synaptic transmission and plasticity have been intensely studied, but their role in coherent function of the circuit has received much less attention, even though glia constitute almost half of all of the cells in the adult human brain (17) and are well-suited for long-range, network-wide signaling. Astrocytes also tile the cortex with near-complete coverage (18, 19), are connected into an extensive syncytium via gap junctions (20, 21), and communicate by intercellular calcium signaling (22), and processes from a single astrocyte can contact up to tens of thousands of synapses (18), making them attractive candidates for mediating neuronal synchronization. Here we describe a role of astrocytes in the cortical circuit, demonstrating their importance in the modulation of neuronal UP states.

Results

UP States Are Network-Wide Events. We performed whole-cell patch clamping of neurons in acute mouse cortical slices from somatosensory area S1. As described (23), we observed spontaneously occurring UP states, synchronized neuronal ensemble activations. In neuronal current clamp recordings, we observed a spontaneous UP state every 5.15 ± 0.27 min (n = 148 UP states, 35 slices). UP state depolarization shifts (20.1 ± 0.6 mV) lasted 1.59 ± 0.08 s and were easily distinguished from excitatory postsynaptic potentials and action potentials by kinetics (Fig. 1*A*). To establish the extent of synchronization during UP states, we performed calcium imaging of hundreds of neurons in the circuit, and observed that many neurons fired action potentials simultaneously during UP states (Fig. 1*A*) (6). Next, we patched two layer 2/3 pyramidal neurons 400- to 600-μm apart and recorded spontaneous activity. UP states recorded from one neuron were always observed in the other neuron (n = 8 slices, 92 UP states), although UP state depolarizations were often subthreshold (Fig. 1*B*). Thus, most, if not all, pyramidal neurons in a cortical region undergo spontaneous UP states together, and recording from individual neurons reflects this.

Stimulation of Individual Astrocytes Increases UP State Number. We next recorded simultaneously from neurons and astrocytes (Fig. 1*C*) in cortical slices, patching a layer 1 astrocyte and a nearby (<200 μm) layer 2/3 pyramidal neuron (Fig. 1 *D* and *E*). Astrocytes were clearly distinguishable from neurons morphologically and electrophysiologically, with smaller somata, more compact and bushy fine processes (Fig. 1*D*) as well as a lower input resistance ($R_{(I)}$ 74.1 ± 5.9 MΩ), a more hyperpolarized resting membrane potential ($V_{(M)}$ −82.9 ± 0.8 mV) than neurons (R_I = 361.5 ± 19.3 MΩ, V_M = −70.7 ± 0.6 mV, $P < 0.001$ for both measures), and a linear current-voltage (IV) curve (Fig. S1*A*). Whereas neurons generated action potentials, astrocytes never did. Biocytin morphological processing revealed that astrocytes were highly connected, as demonstrated by the spread of biocytin across many astrocytes (51.2 ± 5.0 cells), covering a total area of 65.8 × 10^3 ± 5.6 × 10^3 μm^2 (Fig. 1*E*) (n = 12 slices), similar to previous results (24, 25).

Many techniques have been used to activate astrocytes, including mechanical stimulation (26), bath application of agonists (26, 27), uncaging of active compounds (27, 28), and intracellular current injections (29). To activate astrocytes, we first chose to depolarize astrocytes with a patch pipette, so that single astrocytes—and no neurons—were stimulated (Fig. 2*A*). We injected trains of depolarizing current into individual astrocytes with 5 s-long stimulation patterns (300–1,000 pA, 500 ms, 10 times, 150-ms stimulus interval, mean 66.6 ± 7.3 mV depolarization shift) 8.5 s after the start of a trial. Each trial lasted 4 min, as it has been hypothesized that astrocytes may affect neuronal activity on a long timescale (27). "Stimulation trials" (red) were paired with alternating control trials (gray) without depolarization (Fig. 2 *A* and *B*). In 18 slices and 110 trials (mean 6.11 ± 0.9 trials per slice), we observed a striking doubling of UP state frequency after stimulation (Fig. 2*C*) (1.21 ± 0.14 stimu-

Author contributions: K.E.P. and R.Y. designed research; K.E.P. performed research; K.E.P. analyzed data; and K.E.P. and R.Y. wrote the paper.

The authors declare no conflict of interest.

*This Direct Submission article had a prearranged editor.

Freely available online through the PNAS open access option.

[1]To whom correspondence should be addressed. E-mail: kp2248@columbia.edu.

This article contains supporting information online at www.pnas.org/lookup/suppl/doi:10.1073/pnas.1112378108/-/DCSupplemental.

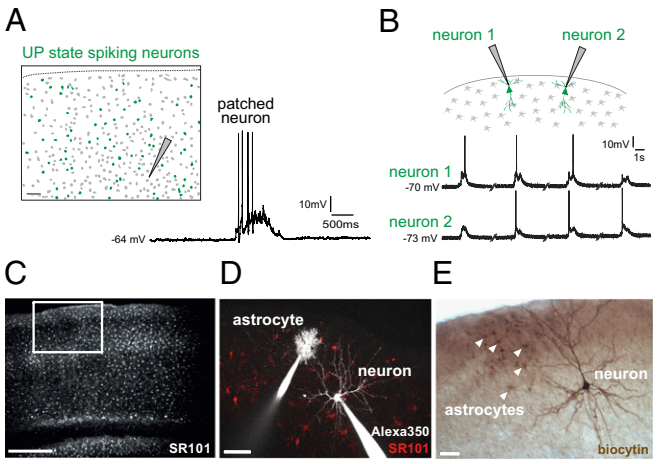

Fig. 1. UP states are synchronous, network-wide events. (*A*) Cortical slice labeled with Fura-2. Cells in green displayed significant calcium increases, corresponding to action potentials, during the UP state recorded in a layer 5 neuron (patched). Gray cells did not change in Fura-2 fluorescence and presumably did not fire action potentials. (*Right*) Recorded UP state. (*B*) Neurons 500-μm apart depolarize synchronously during UP state. Traces are not continuous in time. We never observed an UP state in one neuron but not in the other. Note that each neuron depolarizes during the UP state but does not always spike. (*C*) Two-photon image of astrocytes across all six cortical layers in area S1, labeled with SR101. The white box represents the extent of cortical layers for subsequent imaging. (*D*) Whole-cell patch-clamped astrocyte (layer 1) and pyramidal neuron (layer 2/3) with Alexa 350 (white) in pipettes. Astrocytes labeled with SR101 (red). (*E*) Biocytin-labeled neuron and astrocytes, five of which are marked by arrowheads. These are not the same two cells as in *D*. (Scale bars, 50 μm.)

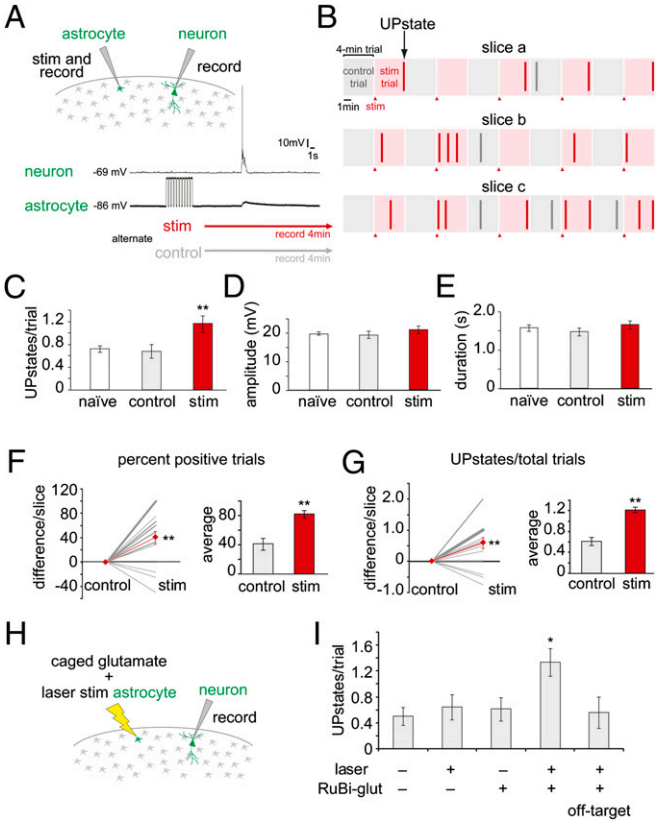

Fig. 2. Stimulation of individual astrocytes increases network UP states. (*A*) Schematic of stimulation experiment. The astrocyte and neuron are patch-clamped and the astrocyte is periodically depolarized ("stim," red). Trials last 4 min; each stimulation trial is matched with a control trial (gray). (*B*) Examples of experimental results. Control and stimulation trials are shown as gray and red boxes, respectively, and UP states as vertical bars (red or gray). (*C–E*) UP states in stimulated (red), control (gray), and naïve (white) trials. (*C*) UP state number, (*D*) amplitude, and (*E*) duration. (*F* and *G*) Slice-by-slice analyses of the same set of experiments. Differences between trial types are shown in the line graphs, with control set at zero. Gray lines represent the average for all trials in an individual slice, and the thickness of the lines represents the number of slices. The average change between two trial types is shown as a red line. Bar graphs show average numbers. (*F*) Trials with at least one UP state are positive trials; percent positive trials are shown. (*G*) Average UP states per trial. (*H*) Schematic of RuBi-glutamate uncaging experiment. (*I*) UP states following astrocyte glutamate uncaging, with laser, caged-compound, and target controls. Errors bars indicate ±SEM. $*P < 0.05$, $**P < 0.01$, paired two-tailed *t* test.

lation vs. 0.61 ± 0.13, $P < 0.01$). There was no significant increase in UP state frequency in control trials compared with slices that had never had any astrocyte stimulation ("naïve"; 0.72 ± 0.06) (Fig. 2*C*). UP state amplitude or duration was similar under all three conditions (Fig. 2 *C–E*). Similar increases in UP state frequencies after stimulation of individual astrocytes were obtained whether slices were labeled with calcium indicators or the astrocyte marker sulforhodamine 101 (SR101) or not (Fig. S1 *B* and *C*). Examining the data slice by slice, we observed that the percentage of trials in each slice with at least one UP state ("positive trials") was also significantly increased in the stimulation trials over controls (Fig. 2*F*) (81.9 ± 5.0% stimulation vs. 41.3 ± 8.1%, $P < 0.01$), in addition to the total number of UP states (Fig. 2 *C* and *G*).

To confirm our results, we stimulated astrocytes with another single-cell resolution method using targeted two-photon uncaging of RuBi-glutamate (30). In these experiments, we recorded from a patched neuron in layer 2/3 following photostimulation of an SR101-labeled astrocyte in layer 1 (Fig. 2*H*). We observed a significant increase in UP state number per trial (1.33 ± 0.18, $n = 18$ trials per condition, $P < 0.05$ compared with unstimulated trials) when uncaging glutamate on an astrocyte, but not during the control trials (−laser,−RuBi = 0.5 ± 0.14; +laser,−RuBi = 0.64 ± 0.19; −laser,+RuBi = 0.61 ± 0.18; +laser,+RuBi, off-target by 15 μm = 0.62 ± 0.2), indicating that the caged compound, laser power, and correct laser positioning on the astrocyte soma are simultaneously necessary to stimulate an individual astrocyte and cause an increase in UP states (Fig. 2*I* and Fig. S1 *D* and *E*). Thus, results from two independent astrocyte stimulation protocols—whole-cell depolarization and laser uncaging—demonstrate that the activation of a *single* astrocyte can have significant effects on the state of large neuronal populations in a circuit, doubling the number of UP states that the circuit generates spontaneously.

Stimulation of Individual Astrocytes Increases Network Astrocytic Calcium Activity. Because astrocytes are coupled through gap junctions, stimulation of one could activate others. However, in dual recordings from neighboring astrocytes, we never observed depolarizations in response to stimulation of another astrocyte ($n = 4$ slices, 12 depolarizations), indicating that the depolarization does not spread across astrocytes via gap-junctional coupling (Fig. S2*B*). To probe how stimulation of an astrocyte might increase UP state frequency, we performed calcium imaging of the local astrocyte population, because astrocytes respond and integrate external signals through calcium release (31). We used the calcium indicator Fluo-4 AM, which exclusively labels astrocytes with our loading protocol (confirmed by SR101), and two-photon imaging of the astrocytes around the patched cell (Fig. 3*A*). Typically, we monitored the activity of 40 to 60 astrocytes when simultaneously recording from an astrocyte and a neuron (Fig. 3 *A–E*). Whether an astrocyte was stimulated or not, a small percentage of the astrocytes exhibited sponta-

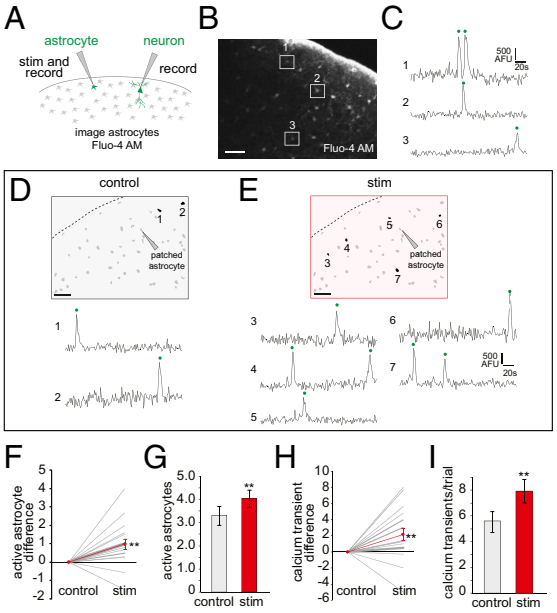

Fig. 3. Stimulation of individual astrocyte increases astrocytic network activity. (*A*) Schematic of experiment. Protocol is the same as in Fig. 2, and astrocyte calcium is imaged with Fluo-4 AM. (*B*) Two-photon micrograph of a Fluo-4-loaded cortical slice. Astrocytes active during the trial are marked by white boxes. (*C*) Calcium traces (unfiltered) from the three cells shown in *B* in a 4-min control trial. Calcium transients are marked by green dots throughout. All traces are at the same scale. AFU, arbitrary fluorescent units. (*D* and *E*) Examples of a matched trial pair. Data from control (*D*) and stimulation (*E*) trials. In both panels, a slice map displays all Fluo-4–loaded astrocytes in gray and all numbered active astrocytes in black. Corresponding calcium traces are set below each map. Note the increase in active astrocytes and total calcium transients in the stimulation trial. (*F*) Difference in active astrocytes in paired trials, with each slice represented by a gray line, as in Fig. 2. The red line is the average difference between the two trial types ($n = 18$ slices). (*G*) Average active astrocytes. (*H*) Difference in total calcium transients (sum of all active astrocytes) in matched trials. The average difference is in red. (*I*) Average total calcium transients. (Scale bars, 50 μm.) $^{**}P < 0.01$, paired two-tailed *t* test.

neous calcium transients characteristic of astrocytes in vivo and in slice (17.7 ± 0.7 s duration, $n = 178$ cells) (Fig. 3 *B–E*) (32–34). Astrocytic calcium transients, associated with release of gliotransmitters (26, 27, 35, 36), were not continuous or oscillatory (1.8 ± 0.1 calcium transients per cell in a 4-min trial; $n = 293$ transients) (Fig. S2*A*). We define "active astrocytes" as those that display a significant increase in intracellular calcium concentration during a trial.

We found significantly more active astrocytes in stimulation trials (4.0 ± 0.3, $n = 225$ cells) compared with controls (3.2 ± 0.4 cells, $n = 178$, $P < 0.01$), indicating that depolarization of a single astrocyte activates the astroglial syncytium (Fig. 3 *F* and *G*) ($n = 18$ slices). Similar results were obtained when counting calcium transients in each active astrocyte (Fig. 3 *H* and *I*) (7.81 ± 0.87 stimulation vs. 5.75 ± 0.82, $P < 0.01$, $n = 413$ transients). Neither the maximum fluorescence change (proportional to the peak calcium concentration) nor the duration of the calcium transients was affected by the stimulation (maximum fluorescence = 1,198 ± 30 stimulation vs. 1,183 ± 34 ΔF arbitrary units, duration = 18.3 ± 0.7 stimulation vs. 17.7 ± 0.7 s, $P > 0.1$ for both measures) (Fig. S2 *B* and *C*), suggesting that the stimulation affected astrocytic calcium in a manner similar to the endogenous spontaneous activation of these cells. The increase in total calcium transients in the stimulation trials was due to the recruitment of more active astrocytes, rather than an increase of calcium transients per active astrocyte, because the average number of calcium transients for each active astrocyte was not different between the two trial types (Fig. S2*C*). In addition, the distance between the two farthest active astrocytes increased as the number of active astrocytes increased, with no difference in stimulated or control trials (Fig. S2*D*), indicating that astrocytes were activated by our stimulation protocol across the entire field of view, rather than in a specific zone. Indeed, this increase in astrocytic calcium was not wave-like in nature, as has been observed in other systems (22, 37). In both trial types, no waves were evident when plotting every transient time as a function of position from the patched astrocyte across the 4-min trial (Fig. S2*E*). Thus, stimulation of a single astrocyte can increase the number of active astrocytes in a spatially distributed manner.

Chelating Astrocytic Calcium Decreases Spontaneous and Stimulated UP States. Because the stimulation methods we used, although spatially precise, are not necessarily physiological, we next sought to determine whether astrocytic activity is causally related to *endogenous* UP state generation in cortex, by interfering with normal astrocytic—but not neuronal—activity. To do this, we introduced the calcium chelator 1,2-bis(2-aminophenoxy)ethane-*N*,*N*,*N*′,*N*′-tetraacetic acid (BAPTA) into a single astrocyte using a patch pipette. In this protocol, one neuron was patched and population astrocyte calcium was imaged (Fluo-4 AM) during four pre-BAPTA trials to obtain a reliable baseline of UP state number and astrocytic calcium activity (Fig. 4 *A–C*, gray). Following the fourth trial, an astrocyte was patched (without positive pressure, to prevent extracellular BAPTA release) with a pipette containing 50 mM BAPTA, and four post-BAPTA trials were carried out (Fig. 4 *A–C*, blue). BAPTA can cross gap junctions between astrocytes and spread through the astrocyte syncytium to inhibit calcium in many astrocytes, as demonstrated by the decrease in calcium transients in neighboring astrocytes (Fig. 4 *B*, *E*, and *F*) (29, 38). We confirmed that astrocytic gap junctions were not blocked when patching with BAPTA by measuring the spread of the biocytin reaction product after fixation (Fig. S3*A*) (80.5 ± 10.2 astrocytes, total area = $109.4 \times 10^3 \pm 11.8 \times 10^3$ μm^2).

Across experiments, the total number of UP states, active astrocytes, and calcium transients was significantly reduced by the introduction of BAPTA (Fig. 4 *C–F*) ($n = 16$ slices). With BAPTA present, active astrocyte and total calcium transients both significantly decreased by ~35–40% by experiment (Fig. 4 *E* and *F*, *Upper*) ($P < 0.05$), whereas UP states decreased by 36% (Fig. 4*D*, *Upper*) ($P < 0.05$). When all experiments were pooled, we observed significant reductions in UP states (50%, 2.3 ± 0.6 decrease), active astrocytes (47%, 4.8 ± 1.9 decrease), and total calcium transients (60%, 13.6 ± 6.0 decrease) (Fig. 4 *D* and *E*, *Lower*) ($P < 0.05$), indicating that UP states are dependent on the level of calcium signaling in astrocytes. Decreases in all three of these measures were observed using lower concentrations (20 mM) of BAPTA in the pipette (Fig. S3 *F–H*). In control experiments, without BAPTA in the astrocyte patch pipette, we observed no reductions in calcium signaling or UP states, indicating that these variables do not simply decrease across time (Fig. S3 *C–E*). Lastly, we confirmed results obtained in the previous calcium imaging experiment, demonstrating that UP state number and astrocytic calcium activity are positively correlated, both before and after BAPTA addition (Fig. S3*B*).

The BAPTA experiments indicated that astrocyte calcium signaling can affect the generation of spontaneous neuronal UP states in cortex. We next wondered whether astrocytic signaling was also important for the generation of UP states that follow astrocytic stimulation. To answer this, we stimulated the patched astrocyte as described earlier in the presence or absence of BAPTA (Fig. 4*G*). In controls, without BAPTA in the pipette, depolarization led to a significant increase in UP state number (Fig. 4*H*; 0.88 ± 0.29 increase), in agreement with our prior results that showed that depolarizing a single astrocyte increases

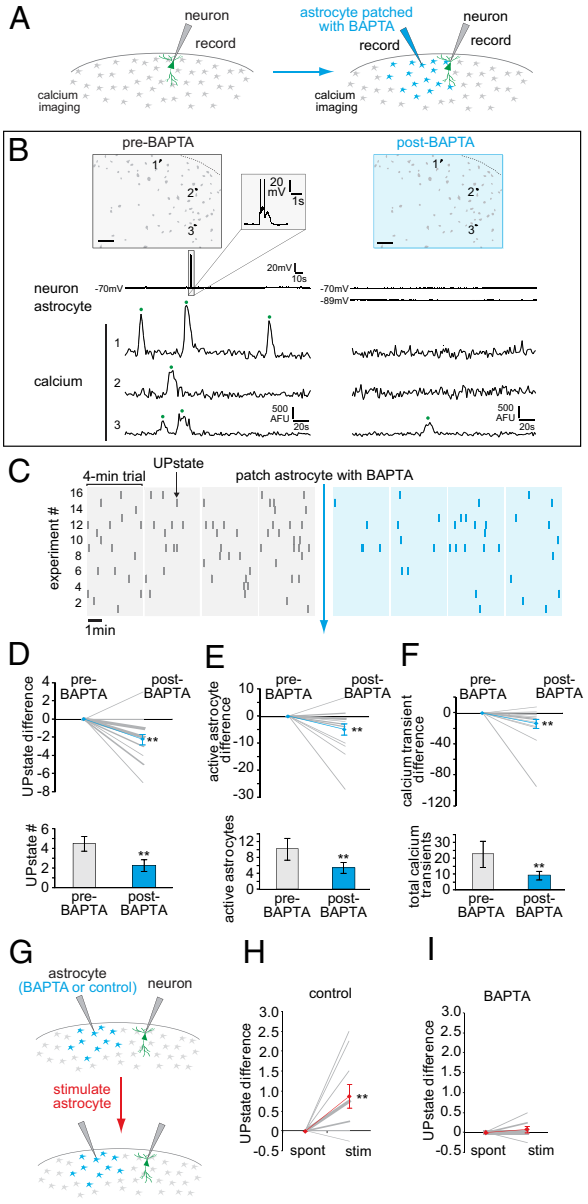

Fig. 4. BAPTA injections into astrocytes inhibit spontaneous and stimulated UP states. (*A*) Schematic of BAPTA experiment. Four 4-min trials are carried out with a patched neuron. Next, a nearby astrocyte is patched with a BAPTA-filled pipette, and four more trials are recorded. The astrocyte is not depolarized. (*B*) One representative trial from each of the two conditions pre-BAPTA and post-BAPTA. An astrocyte calcium map shows the same three cells (all active pre-BAPTA) in both trials. Corresponding electrophysiology and calcium imaging from the two trials, with calcium transients marked by a green dot. (*C*) UP states (ticks) from 16 experiments under pre-BAPTA (gray) and post-BAPTA (blue) conditions. (*D–F*) *Upper* graphs show differences between conditions. Pre-BAPTA levels are set at zero, and data from each condition are summed across all four trials. Average difference values are displayed as blue lines. Bar graphs display average raw numbers for UP states (*D*), active astrocytes (*E*), and calcium transients (*F*) (n = 16 slices). (*G*) Schematic of stimulation experiment in BAPTA. After the last trial, the patched astrocyte is stimulated. The same protocol is followed in the control experiment (Fig. S3), with no BAPTA in the astrocyte pipette. (*H* and *I*) UP state difference upon stimulation without (*H*) and with (*I*) BAPTA in the astrocyte syncytium. (Scale bars, 50 μm.) $^{**}P < 0.01$, paired two-tailed t test.

UP states (Fig. 2). In contrast, when BAPTA spread through the astrocyte network, the stimulation of the astrocyte did not significantly increase UP states (Fig. 4*I*) (0.08 ± 0.07). Thus, astrocyte calcium activity affects the generation of both spontaneous and astrocyte-stimulated UP states, indicating that these two kinds of UP states may be mediated by a common mechanism. Further, the result that stimulation-triggered UP states were inhibited when BAPTA was present intracellularly through the astrocyte syncytium likely excludes the possibility that the depolarization simply raises the local concentration of K^+ around the stimulated astrocyte to generate UP states.

Purinergic and Glutamatergic Signaling Regulate UP State Generation. We next focused on mechanisms that control astrocyte regulation of UP states. After confirming normal UP state activity in each slice, we bath-applied pharmacological agents that affect astrocytes and their targets and measured UP states and astrocyte calcium activity (Fig. 5 *A* and *B*). We found that agents that affected glutamatergic or purinergic signaling had significant effects on UP states. The AMPA-R inhibitor 6-cyano-7-nitroquinoxaline-2,3-dione (CNQX) (0.2 ± 0.11, n = 15 trials) and A_1 adenosine receptor antagonist cyclopentyltheophylline (CPT) (0.35 ± 0.16, n = 22) both significantly decreased UP states, whereas the glutamate transporter inhibitor dihydrokainate (DHK) (4.57 ± 0.57, n = 10) and P2R antagonists Pyridoxalphosphate-6-azophenyl-2′,4′-disulfonic acid (PPADS) (1.17 ± 0.21, n = 28) and suramin (1.71 ± 0.26, n = 23) significantly increased UP states (0.74 ± 0.08, n = 97) (Fig. 5*A*). Other reagents—2-Methyl-6-(phenylethynyl)pyridine (MPEP) (mGluR5 antagonist; 0.8 ± 0.1, n = 10),

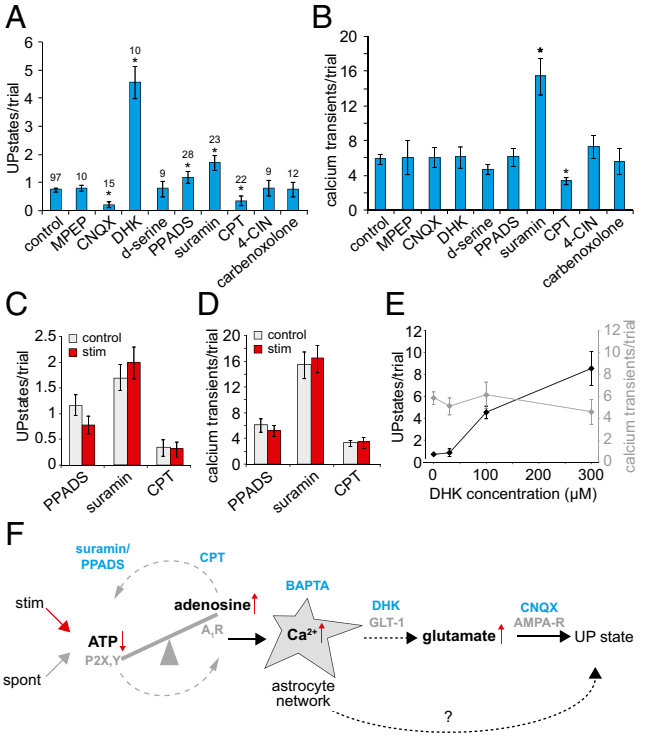

Fig. 5. Purinergic and glutamatergic signaling regulate UP states and astrocyte calcium. (*A* and *B*) Average UP states (*A*) and calcium transients (*B*) in 4-min trials in control (ACSF; leftmost bar) and various pharmacological treatments. Concentrations are indicated in *Experimental Procedures*. 100 μM DHK was used in *A* and *B*. (*C* and *D*) Average UP states and calcium transients in control (gray) and alternating stimulation (red) trials for PPADS, suramin, and CPT. There was no significant difference between control and stimulation trials. The n values are the same as in *A*. (*E*) Average UP states (black, *Left y* axis) and calcium transients (gray, *Right y* axis) during application of varying concentrations of DHK. (*F*) Diagram of results and a possible model for astrocyte-induced UP states. Errors bars indicate ±SEM. $^{*}P < 0.05$, unpaired two-tailed t test.

D-serine (0.78 ± 0.28, $n = 9$), alpha-cyano-4-hydroxycinnamate (4-CIN) (lactate transporter inhibitor; 0.8 ± 0.29, $n = 9$), and carbenoxolone (gap-junction blocker; 0.75 ± 0.25, $n = 12$)—had no effect on UP states. However, purinergic drugs were the only ones with an effect on astrocyte calcium signaling, with suramin application leading to an increase in calcium transients (15.43 ± 2.09) (Fig. 5*B*) and active astrocytes (4.35 ± 0.56) (Fig. S4) and CPT decreasing both measures (3.33 ± 0.42) (Fig. 5*B*) (1.66 ± 0.22) (Fig. S4) compared with controls (5.88 ± 0.59 transients and 2.66 ± 0.21 active astrocytes). PPADS and suramin inhibit a broad range of P2 receptors, although suramin inhibits both P2X and P2Y receptors (ionotropic and metabotropic, respectively), which may account for the observation that calcium activity remained unchanged in slices bathed in PPADS (39). The different results obtained with the P2 receptor inhibitors could be explained by the fact that we carried out imaging at the soma, whereas PPADS might affect astrocytic processes. Another possibility could be a differential inhibition (spatial or temporal) of P2X receptors with PPADS compared with suramin. Nonetheless, reagents that block ATP and adenosine signaling lead to opposite effects in the cortical circuit, indicating that the regulation and balance of purinergic signaling link astrocytic activity to UP state generation.

To confirm that purinergic signaling is linked to astrocyte-triggered UP states, we carried out alternating control and stimulation trials as earlier, in the presence of purinergic inhibitors. We found no increase in UP states, calcium transients, and active astrocytes in stimulation and control trials (Fig. 5 *C* and *D* and Fig. S4), which is markedly different from results found in control experiments in which stimulation caused significant increases in all measures (Figs. 2*C* and 3 *G–I*). These results indicate that suramin, PPADS, and CPT occlude effects of stimulation, suggesting that purinergic signaling is an upstream step in astrocyte-modulated UP state generation. In addition, the opposing effects of inhibiting ATP and adenosine receptors point to the balance of ATP and adenosine signaling as important in the regulation of spontaneous network UP states (Fig. 5*F*). Because astrocytes release ATP which can accumulate as adenosine, these molecules also may act directly on pre- or postsynaptic P2 receptors to act as negative or positive regulators of network UP states, respectively (40, 41).

Finally, our data show that altering glutamatergic signaling affects UP state generation but not astrocytic calcium signaling, suggesting that astrocytes regulate extracellular glutamate either during a downstream step in astrocyte UP state generation or through a different pathway (Fig. 5 *A* and *B*). We tested whether astrocyte-specific glutamate regulation could influence UP state number by examining UP states in varying concentrations of the astrocytic glutamate transporter inhibitor DHK. Increased levels of DHK lead to increased UP states, with no change in calcium transients, indicating that astrocyte glutamate transporters can tune the necessary spatiotemporal levels of extracellular glutamate in the cortex to modulate UP states (Fig. 5*E*).

Discussion

Our results demonstrate a profound effect that astrocytes can have on the state of the neuronal circuit by regulating the generation of neuronal UP states. This supports the idea that astrocytes are active partners in the computations of the circuit. The stimulation of a *single* astrocyte can activate the astrocytic network and double the number of UP states, whereas inhibition of astrocytic activity with BAPTA blocks half of the UP states. Our data also indicate that multiple astrocytes in the circuit must be active to exert their effects on neuronal UP states. Although we do not observe waves in our system, a signal—likely the accumulation of adenosine—from the stimulated astrocyte and other activated astrocytes is likely to be spread through the network. Thus, it may be necessary to have a threshold number of activated astrocytes across a spatially distributed area in order for these cells to exert an effect on the neurons in the circuit. Moreover, our BAPTA data indicate that astrocyte calcium transients are causally linked to the entry of the neuronal network into UP states, regardless of whether the UP states were spontaneous or astrocyte-evoked, suggesting that spontaneous and astrocyte-triggered UP states share a common mechanism.

The precise mechanisms by which the highly coordinated spontaneous synaptic activations of UP states occur are still unclear. We show that purinergic signaling can regulate both astrocytic network-level calcium signaling and neuronal network UP states. The effects of single-astrocyte stimulation are occluded during exposure to purinergic inhibitors, indicating that purinergic signaling is important at an early, upstream step of UP state generation (Fig. 5*F*). This may not be unexpected because ATP-triggered release of calcium from astrocytic internal stores is important in calcium wave propagation (42, 43) and astrocytes communicate via purinergic chemical coupling (44). Because we obtained opposite results using antagonists of ATP and adenosine, and these molecules are enzymatically linked to each other, spontaneous UP states may occur when the extracellular balance of these two molecules tips toward more adenosine in the circuit (39). We hypothesize that astrocyte stimulation alters the ATP/adenosine signaling balance in the circuit to regulate the cortical network state. Both neurons and glia express purinergic receptors, so it is difficult to disentangle whether direct purinergic signaling on astrocytes, neurons, or a combination of both is responsible for the effects we observe or, more generally, in mechanistic studies of astrocytes. The development of more specific pharmacological or molecular tools could further the dissection of these mechanisms.

Glutamate receptor blockers inhibit spontaneous UP state generation (6, 9). Consistent with this, we find that blockade of astrocyte glutamate transporters increases the number of UP states. Activation of the astrocytic network from purinergic signals could lead to release of calcium from internal stores across astrocytes in the local circuit, which then could trigger cortical UP states via the regulation of glutamate by activated astrocytes. By demonstrating that we can tune UP states using reagents that affect astrocytic glutamate signaling, we link astrocytic regulation of glutamate to UP state generation (Fig. 5*F*). Although our experiments target astrocytic glutamate transporters, other mechanisms of glutamate release, including vesicular, are also consistent with our results.

Since UP and DOWN states are the basis of the oscillatory activity observed during slow-wave sleep (10, 11), our finding that astrocytes are causally linked to UP states indicates that astrocytes are mechanistically involved in sleep, consistent with reports of sleep perturbations in mice lacking astrocytic vesicular release (45, 46). But, in addition to sleep, UP states have been implicated in other types of circuit functions including attention, memory consolidation, and resting state activity (6, 7, 12–14). Thus, our work indicates that, by regulating UP states, astrocytic activity could also play an important modulatory role in these circuit processes.

Experimental Procedures

Slice Preparation and Electrophysiology. In accordance with Columbia's Institutional Animal Care and Use Committee, coronal neocortical slices (400-μm thick) from postnatal day (P)13 to P15 C57/BL6 mice were cut with a vibratome (VT1200S; Leica) in ice-cold cutting solution of 27 mM $NaHCO_3$, 1.5 mM NaH_2PO_4, 222 mM sucrose, 2.6 mM KCl, 2 mM $MgSO_4$, and 2 mM $CaCl_2$. Slices were incubated for 30 min at 32 °C in standard, continuously aerated (95% O_2/5% CO_2) artificial cerebrospinal fluid (ACSF) containing 123 mM NaCl, 3 mM KCl, 26 mM $NaHCO_2$, 1 mM NaH_2PO_4, 10 mM dextrose, 2 mM $CaCl_2$, and 2 mM $MgSO_4$. For dye loading, we deposited slices in a Petri dish (35 × 10 mm) with 2 mL ACSF. An aliquot of 50 μg Fluo-4 AM or Fura-2 AM (Invitrogen) was prepared in 10 μL DMSO and 2 μL Pluronic F-127 (Invitrogen), shaken for 5 min, and pipetted into the solution with slices. The dish was ventilated with 95% O_2/5% CO_2 and affixed to the bottom of a larger Petri

dish kept humid with a wet Kimwipe and placed in a 37 °C slide warmer for 15 min. To the petri dish, we added 20 μM sulforhodamine 101 (Invitrogen) and incubated for 10 more min. Slices were transferred back into the incubation chamber until experiments were performed. In all experiments, continuously aerated, standard ACSF (concentrations above) was used.

Whole-cell patch-clamp recording was performed using electrodes with a resistance of 5 to 8 MΩ and an intracellular solution containing 135 mM K-methylsulfate, 10 mM KCl, 10 mM Hepes, 5 mM NaCl, 2.5 mM Mg-ATP, 0.3 mM Na-GTP, and 2 mg/mL mM biocytin (pH 7.3). For BAPTA experiments, varying concentrations of BAPTA (Invitrogen) were added to the solution. For pharmacological experiments, the following bath concentrations were used: MPEP (50 μM; Tocris), CNQX (10 μM; Sigma), DHK (30–300 μM), D-serine (100 μM; Tocris), PPADS (20 μM; Tocris), suramin (50 μM), CPT (4 μM; Sigma), 4-CIN (500 μM; Sigma), and carbenoxolone (50 μM; Sigma). For pharmacological experiments, reagents were perfused for 5 min before experimental trials. Experiments were conducted at 25 °C. Offline analysis was performed using MATLAB (MathWorks).

Imaging. Two-photon imaging was performed on a custom-made two-photon microscope (47) with a tunable titanium:sapphire laser (Chameleon; Coherent). The upright microscope (Olympus BX50WI) was equipped with a 40×, 0.8 NA objective. The laser was tuned to 800 nm, with 510/40 and 605/20 emission filters (Chroma) to image Fluo-4 and SR101, respectively. Images were taken at 800 × 600 pixels with a frame rate of 1.55 s, detected with a photomultiplier tube (Hamamatsu), and collected with Olympus FluoView software. For Fluo-4 imaging, laser power was kept below 70 mW at the periscope, with power modulated by a Pockels cell (Conoptics). Calcium imaging analysis was performed using custom-written MATLAB software.

For biocytin imaging, slices were kept overnight in 2% paraformaldehyde in 0.1 M phosphate buffer (PB) at 4 °C, rinsed in 0.1 M PB, placed in 30% sucrose solution (30 g sucrose in 50 mL ddH_2O and 50 mL 0.24 M PB) for 2 h, and frozen on dry ice in tissue-freezing medium. Slices were kept overnight at −80 °C and then defrosted and rinsed with PB. Standard DAB staining protocols were performed, and slices were mounted onto slides. Neurons and astrocytes that were biocytin-labeled were viewed with a 20×, 0.5 NA objective on an Olympus IX71 inverted light microscope.

Glutamate Uncaging. For uncaging experiments, a laser power protocol was determined such that stimulation of the astrocyte soma in the presence of 300 μM RuBi-glutamate (Tocris) caused an increase in astrocytic calcium (Fluo-4 imaging) but not in the absence of RuBi-glutamate (175 mW before periscope, 800 nm, 6 subtargets, 8 ms per subtarget). Alternating 4-min trials with and without laser stimulation were carried out first in the absence of RuBi-glutamate and then in the presence following the addition of caged compound in the dark. For each slice, a stimulation trial in the presence of the caged compound, but ∼20 μm off the astrocyte soma, was carried out.

ACKNOWLEDGMENTS. We thank R.Y. laboratory members for help; S. Yeonsook for anatomical reconstructions; M. Dar for help with mice and software; and E. Fino, H. Hirase, and A. Woodruff for comments. This work was supported by The Patterson and Revson Foundations, The Kavli Institute for Brain Science, and the National Eye Institute.

1. Haider B, McCormick DA (2009) Rapid neocortical dynamics: Cellular and network mechanisms. *Neuron* 62(2):171–189.
2. Harris KD, Csicsvari J, Hirase H, Dragoi G, Buzsáki G (2003) Organization of cell assemblies in the hippocampus. *Nature* 424:552–556.
3. Hebb DO (1949) *The Organization of Behavior: A Neuropsychological Theory* (Wiley, New York).
4. Lorente de No R (1938) Analysis of the activity of the chains of internuncial neurons. *J Neurophysiol* 1:207–244.
5. Brecht M, Sakmann B (2002) Dynamic representation of whisker deflection by synaptic potentials in spiny stellate and pyramidal cells in the barrels and septa of layer 4 rat somatosensory cortex. *J Physiol* 543(Pt 1):49–70.
6. Cossart R, Aronov D, Yuste R (2003) Attractor dynamics of network UP states in the neocortex. *Nature* 423:283–288.
7. Kenet T, Bibitchkov D, Tsodyks M, Grinvald A, Arieli A (2003) Spontaneously emerging cortical representations of visual attributes. *Nature* 425:954–956.
8. Petersen CC, Grinvald A, Sakmann B (2003) Spatiotemporal dynamics of sensory responses in layer 2/3 of rat barrel cortex measured in vivo by voltage-sensitive dye imaging combined with whole-cell voltage recordings and neuron reconstructions. *J Neurosci* 23:1298–1309.
9. Sanchez-Vives MV, McCormick DA (2000) Cellular and network mechanisms of rhythmic recurrent activity in neocortex. *Nat Neurosci* 3:1027–1034.
10. Steriade M, Nuñez A, Amzica F (1993) Intracellular analysis of relations between the slow (< 1 Hz) neocortical oscillation and other sleep rhythms of the electroencephalogram. *J Neurosci* 13:3266–3283.
11. Steriade M, Timofeev I, Grenier F (2001) Natural waking and sleep states: A view from inside neocortical neurons. *J Neurophysiol* 85:1969–1985.
12. Cowan RL, Wilson CJ (1994) Spontaneous firing patterns and axonal projections of single corticostriatal neurons in the rat medial agranular cortex. *J Neurophysiol* 71(1): 17–32.
13. Hahn TT, Sakmann B, Mehta MR (2006) Phase-locking of hippocampal interneurons' membrane potential to neocortical up-down states. *Nat Neurosci* 9:1359–1361.
14. Biswal B, Hudetz AG, Yetkin FZ, Haughton VM, Hyde JS (1997) Hypercapnia reversibly suppresses low-frequency fluctuations in the human motor cortex during rest using echo-planar MRI. *J Cereb Blood Flow Metab* 17:301–308.
15. Fox MD, Raichle ME (2007) Spontaneous fluctuations in brain activity observed with functional magnetic resonance imaging. *Nat Rev Neurosci* 8:700–711.
16. Greicius MD, Krasnow B, Reiss AL, Menon V (2003) Functional connectivity in the resting brain: A network analysis of the default mode hypothesis. *Proc Natl Acad Sci USA* 100:253–258.
17. Barres BA (2008) The mystery and magic of glia: A perspective on their roles in health and disease. *Neuron* 60:430–440.
18. Bushong EA, Martone ME, Jones YZ, Ellisman MH (2002) Protoplasmic astrocytes in CA1 stratum radiatum occupy separate anatomical domains. *J Neurosci* 22(1): 183–192.
19. Halassa MM, Fellin T, Takano H, Dong JH, Haydon PG (2007) Synaptic islands defined by the territory of a single astrocyte. *J Neurosci* 27:6473–6477.
20. Brightman MW, Reese TS (1969) Junctions between intimately apposed cell membranes in the vertebrate brain. *J Cell Biol* 40:648–677.
21. Tani E, Nishiura M, Higashi N (1973) Freeze-fracture studies of gap junctions of normal and neoplastic astrocytes. *Acta Neuropathol* 26(2):127–138.
22. Cornell-Bell AH, Finkbeiner SM, Cooper MS, Smith SJ (1990) Glutamate induces calcium waves in cultured astrocytes: Long-range glial signaling. *Science* 247:470–473.
23. MacLean JN, Watson BO, Aaron GB, Yuste R (2005) Internal dynamics determine the cortical response to thalamic stimulation. *Neuron* 48:811–823.
24. Houades V, Koulakoff A, Ezan P, Seif I, Giaume C (2008) Gap junction-mediated astrocytic networks in the mouse barrel cortex. *J Neurosci* 28:5207–5217.
25. Robinson SR, Hampson EC, Munro MN, Vaney DI (1993) Unidirectional coupling of gap junctions between neuroglia. *Science* 262:1072–1074.
26. Angulo MC, Kozlov AS, Charpak S, Audinat E (2004) Glutamate released from glial cells synchronizes neuronal activity in the hippocampus. *J Neurosci* 24:6920–6927.
27. Fellin T, et al. (2004) Neuronal synchrony mediated by astrocytic glutamate through activation of extrasynaptic NMDA receptors. *Neuron* 43:729–743.
28. Perea G, Araque A (2005) Properties of synaptically evoked astrocyte calcium signal reveal synaptic information processing by astrocytes. *J Neurosci* 25:2192–2203.
29. Kang J, Jiang L, Goldman SA, Nedergaard M (1998) Astrocyte-mediated potentiation of inhibitory synaptic transmission. *Nat Neurosci* 1:683–692.
30. Fino E, et al. (2009) RuBi-glutamate: Two-photon and visible-light photoactivation of neurons and dendritic spines. *Front Neural Circuits* 3:1–9.
31. Peuchen S, Clark JB, Duchen MR (1996) Mechanisms of intracellular calcium regulation in adult astrocytes. *Neuroscience* 71:871–883.
32. Nett WJ, Oloff SH, McCarthy KD (2002) Hippocampal astrocytes in situ exhibit calcium oscillations that occur independent of neuronal activity. *J Neurophysiol* 87:528–537.
33. Nimmerjahn A, Kirchhoff F, Kerr JN, Helmchen F (2004) Sulforhodamine 101 as a specific marker of astroglia in the neocortex in vivo. *Nat Methods* 1(1):31–37.
34. Takata N, Hirase H (2008) Cortical layer 1 and layer 2/3 astrocytes exhibit distinct calcium dynamics in vivo. *PLoS One* 3:e2525.
35. Jourdain P, et al. (2007) Glutamate exocytosis from astrocytes controls synaptic strength. *Nat Neurosci* 10:331–339.
36. Navarrete M, Araque A (2008) Endocannabinoids mediate neuron-astrocyte communication. *Neuron* 57:883–893.
37. Hoogland TM, et al. (2009) Radially expanding transglial calcium waves in the intact cerebellum. *Proc Natl Acad Sci USA* 106:3496–3501.
38. Gómez-Gonzalo M, et al. (2010) An excitatory loop with astrocytes contributes to drive neurons to seizure threshold. *PLoS Biol* 8:e1000352.
39. Fields RD, Burnstock G (2006) Purinergic signalling in neuron-glia interactions. *Nat Rev Neurosci* 7:423–436.
40. Zhang JM, et al. (2003) ATP released by astrocytes mediates glutamatergic activity-dependent heterosynaptic suppression. *Neuron* 40:971–982.
41. Pascual O, et al. (2005) Astrocytic purinergic signaling coordinates synaptic networks. *Science* 310(5745):113–116.
42. Bowser DN, Khakh BS (2007) Vesicular ATP is the predominant cause of intercellular calcium waves in astrocytes. *J Gen Physiol* 129:485–491.
43. Cotrina ML, Lin JH, López-García JC, Naus CC, Nedergaard M (2000) ATP-mediated glia signaling. *J Neurosci* 20:2835–2844.
44. Anderson CM, Bergher JP, Swanson RA (2004) ATP-induced ATP release from astrocytes. *J Neurochem* 88:246–256.
45. Fellin T, et al. (2009) Endogenous nonneuronal modulators of synaptic transmission control cortical slow oscillations in vivo. *Proc Natl Acad Sci USA* 106:15037–15042.
46. Halassa MM, et al. (2009) Astrocytic modulation of sleep homeostasis and cognitive consequences of sleep loss. *Neuron* 61:213–219.
47. Nikolenko V, Poskanzer KE, Yuste R (2007) Two-photon photostimulation and imaging of neural circuits. *Nat Methods* 4:943–950.